

Anomalous diffusion in fractal globules

M.V. Tamm^{1,2}, L.I. Nazarov¹, A.A. Gavrilov^{1,3}, A.V. Chertovich¹

¹Physics Department, Moscow State University, 119991, Moscow, Russia

²Department of Applied Mathematics, National Research University Higher School of Economics, 101000, Moscow, Russia

³Institute for Advanced Energy Related Nanomaterials, University of Ulm, D-89069, Ulm, Germany

(Dated: February 12, 2019)

Fractal globule state is widely believed to be the best known model to describe the chromatin packing in the eucaryotic nuclei. Here we provide a scaling theory and dissipative particle dynamics (DPD) computer simulation for the thermal motion of monomers in the fractal globule state. We show this motion to be subdiffusive described by $\langle X^2(t) \rangle \sim t^{\alpha_F}$ with α_F close to 0.4. We also suggest a novel way to construct a fractal globule state in computer simulation, and provide simulation evidence supporting the conjecture that different initial entanglement-free states of a polymer chain converge as they are thermally annealed.

PACS numbers: 05.40.Fb, 82.35.Lr, 82.35.Pq, 87.15.ap, 87.15.H-, 87.15.Vv

The question of how genetic material is packed inside the eucaryotic nucleus is one of the most challenging in contemporary molecular biology. Indeed, not only are 2 meters of DNA packed inside a tiny volume of several thousands μm^3 but its packing has some striking biological properties. It is well known (see, e.g. [1]) that there exist very distinct chromosome territories in the nucleus, that the chromosomes get quite easily unentangled when the cell prepares to mitosis, that parts of the *chromatin* (that is to say, a composite polymer fiber consisting of ds-DNA and associated *histone* proteins[2]) can easily loop out from the dense state, and that different parts of chromatin can find each other diffusively strikingly fast in e.g. so-called promoter-enhancer interactions. All these properties differ very much from the properties of equilibrium liquid globules known from classical polymer physics (see, e.g. [3, 4]). Indeed, the equilibrium globule states of such a long fiber implies so much entanglement that it would have prevented DNA from carrying out its biological functions on any reasonable time-scale [5].

The question of how the chromatin is stabilized in the nucleus has remained wide open for a long time, in the recent 25 years it has been attacked by various authors mostly implying either some *ad hoc* biological mechanism of stabilization [6–11] or stabilization by topological interactions preventing the chromatin chain from entangling itself on biological timescales [5, 12–14]. The latter point of view, so-called fractal globule approach, relies heavily on the analogy between chromatin state and other topologically-governed polymer states, e.g. the crumpled globule [12, 15–17] formed on the early stages of a polymer coiled collapse, or the melt of non-concatenated polymer rings [18–22].

In recent years, the development of novel experimental techniques has made possible a very deep insight into the statistical properties of chromatin packing and dynamics. FISH method [23] allows one to measure the spatial size R of a subchain as a function of its length n , while the Hi-C method (genome-wide chromosome conformation capture method) [13, 24] is used to collect data

on the parts of genome which are located spatially close to each other. Both these methods show that the statistics of chromatin packing is quite far from that expected in equilibrium polymer globules. In particular, a gradual decay of the average probability of contact with growing genomic distance between chromatin regions measured in Hi-C experiments roughly obeys a power law with exponent γ between 1 and 1.1 for various organisms studied [13, 25–27], while $\gamma = 1.5$ is expected in equilibrium globule.

All these experimental results are in compliance with a hypothesis that the chromatin material in the nucleus of a human cell is packed in the form of a fractal globule, which is why the “topological” theory of chromatin packing seems to gain more and more ground lately.

Following [14, 15], let us outline the most important properties of the fractal globule state. First of all, the fractal globule is indeed a fractal with dimensionality equal to 3. That is to say, on all length scales the typical spatial distance R between monomers is proportional to the genomic distance s between them as $R \sim s^{1/D_f} = s^{1/3}$ contrary to the case of a usual equilibrium globule, where $R \sim s^{1/2}$ for $s < L^{2/3}$ and $R \sim \text{const}$ for $s > L^{2/3}$ with L being the full contour length of the chain. The probability p for the two monomer to be in spatial proximity of each other at any given time is $p \sim s^{-\gamma}$ with the exponent γ , for which the estimates range from 1 [13, 14, 28] to 1.09 [22], these estimates are in good agreement with the results obtained from the experimental Hi-C maps.

Second, there are no entanglements in the fractal globule contrary to the equilibrium one. Different parts of the DNA can therefore move independently, there are no topological constraints preventing the relative displacement of different parts of the chain with respect to each other. Due to this feature the parts of DNA can easily fold out from the fractal globule conformation and form extended loops, and then retract back to refold into the dense fractal globular state. Finally, the fractal glob-

ule has a distinct territorial organization: parts of the genome close to each other along the chromosome are close to each other in space as well. At the same time, these compact distinct domains have very developed surface.

It is important to note that, although the fractal globule state is expected to be rather long-living for linear polymer chains and equilibrium for non-concatenated polymer rings, the question of how to prepare a fractal state with long-living stable properties is still a matter of large controversy. Many different algorithms to prepare a fractal globule in computer simulations have been suggested [11, 13, 30–32], most of them appear to be evolving in time rather rapidly when the simulation starts. To avoid this controversy in our computer simulations we used two different algorithms to prepare initial fractal states in what follows, then annealed them for some time before starting any measurements. The observed convergence of the results obtained from two different initial states suggests that indeed there exists a unique meta-stable fractal globule state corresponding to a partial equilibrium of the polymer chain which respects the absence of topological entanglements.

Contrary to the static properties, the dynamics of a fractal globule state, which is a focus of this paper, has been less studied so far. It is clear that the self-diffusion in the fractal globule should be faster than in the equilibrium one due to the absence of entanglements. In several recent papers (e.g. [11, 33]) the Rouse dynamics of the fractal state is assumed in order to estimate the relaxation times of the chain as a whole. However, it is clear that Rouse dynamics relies heavily on the Gaussian properties of the moving chain, so it cannot be directly applicable to fractal globules whose conformations have very different statistical properties.

Experimentally, the dynamics of chromatin in the nuclei has been studied on many length scales, although most results tend to be qualitative rather than quantitative. On the comparatively small length scales, in the series of works [34–36] the dynamics of telomeres (end-regions of chromosomes) is studied extensively, and the subdiffusion $\langle X^2(t) \rangle \sim t^\alpha$ (where $X(t) = R(t) - R(t=0)$ is the telomer displacement up to time t) is reported with α close to 0.4, contrary to the Rouse value of 1/2. In what follows we present a scaling theory and computer simulations of the self-diffusion in a fractal globule state resulting in a subdiffusive motion with a very similar exponent.

Consider a polymer chain in a state with fractal dimension d_f . Let monomers of this chain perform a thermal motion. One can expect then the mean square displacement of a monomer $\langle X^2(t) \rangle$ to grow subdiffusively with time t :

$$\langle X^2(t) \rangle \sim t^\alpha \sim D(X)t, \quad (1)$$

where $\alpha < 1$ is some scaling exponent. The motion of the monomers is subdiffusive due to the fact that they cannot

move independently, the displacement of each unit of the chain is suppressed by its connection to the surrounding chain. In the last equation of (1) we allow for that by formally introducing a *displacement-dependent diffusion coefficient* $D(X)$. Indeed, a monomer unit drifting in space by the distance X cannot move independently from other units of the chain, it has to drag part of the chain together with itself. The size of this part of the chain, so-called blob, which moves collectively with the monomer under consideration grows with growing displacement, and the $D(X)$ has a meaning of the effective diffusion coefficient of such a collectively moving blob. If the chain conformation is indeed fractal then the monomer displacement is the only characteristic scale of the problem, and the blob size is obliged to be of the same order of magnitude as X . We see therefore that the spatial size of the displacement blob grows as

$$R_b(t) \sim X(t) \sim t^{\alpha/2}, \quad (2)$$

and the number of monomer units $g(t)$ in the blob grows as

$$g(t) \sim (R_b(t)/a)^{d_f} \sim t^{d_f \alpha/2}, \quad (3)$$

where a is the microscopic scale of the system (e.g., typical size of the monomer unit).

Now, to close the set of equations (1)-(3) we are to make an assumption concerning the dependence of the effective diffusion coefficient of the blob $D(X)$ on its size g . Such a dependence is known [3, 4, 37] to be controlled by the concrete details of the state dynamics. In particular, it is very sensitive to the presence of, on the one hand, topological entanglements and, on the other hand, hydrodynamic interactions in the system (the former depresses the motion, while the latter enhances it). In the case of a fractal globule, however, the entanglements are absent by definition. Moreover, one can expect that, since the fractal blob is a random and evolving dense object, the monomers on its surface are independently of each other subject to friction with the surroundings, while monomers in the bulk of the blob move collectively and do not participate in the friction similarly to the inner monomers of a regular globule. We expect therefore the X -dependent diffusion coefficient to be inversely proportional to the number of monomers on the surface of the blob:

$$D(X) \sim \frac{D_0}{S(t)/S_0}, \quad (4)$$

where D_0 and S_0 are the microscopic parameters (roughly the diffusion coefficient and a surface area of a single monomer unit), and $S(t) \sim S_0[g(t)]^\beta$ is the surface area of the blob. The exact value of exponent β (which is connected to γ mentioned above by the equality $\beta + \gamma = 2$ [38]) is a matter of some controversy. Theoretically, simple mean-field calculation gives [13] $\beta = 1$, while a more sophisticated analysis leads to a conjecture [22] $\beta \approx 0.91$.

Meanwhile, the analysis of numerical data gives results from $\beta \approx 0.93$ [39] to $\beta = 1$ [28]. Accordingly, in what follows we assume β to belong to the $0.91 < \beta < 1$. range.

Combining equations (1)-(4) one gets finally

$$\begin{aligned} \langle X^2(t) \rangle &\sim t^\alpha \sim \frac{D_0}{S_0} \frac{t}{S(t)} \sim t^{1-d_f\beta\alpha/2} \\ \alpha &= 1 - d_f\beta\alpha/2 \\ \alpha &= \frac{2}{2+d_f\beta} \end{aligned} \quad (5)$$

which for $d_f = 2$ and $\beta = 1$ (i.e., for a Gaussian polymer coil) returns the usual Rouse result $\alpha_R = 1/2$, while for the fractal globule with $d_f = 3$ formula (5) gives $\alpha_F \approx 0.42$ for $\beta \approx 0.91..0.94$ or $\alpha_F = 0.4$ for $\beta = 1$. Note, that similar predictions for the subdiffusive dynamics in different fractal systems have been mentioned in the literature, e.g. in [40] a formula equivalent to (5) is used for the case of Rouse-like self-diffusion of a swollen polymer coil with $d_f = 1/\nu \approx 1.70$, $\beta = 1$.

The natural reference state to compare a fractal globule with is, of course, a usual entangled equilibrium globule. It is known that there the self-diffusion of monomer units is described by the Rouse exponent $\alpha_R = 1/2$ on short time scales, when displacement is smaller than the typical size of the entanglement blob. For larger time and length scales the entanglements pay crucial role and the scaling theory [4] predicts $\alpha_{\text{ent}} = 1/4$.

To check the predictions of the scaling theory we held out extensive computer simulations based on the dissipative particle dynamics (DPD) technique which is known [41, 42] to correctly reflect dynamics of dense polymer systems. The polymer model we use (see [32] for more details) consists of renormalized monomers with the size of order of the chromatin persistence length, the volume interactions of these monomers are chosen in a way that guarantees the absence of chain self-intersections, the entanglement length for the parameters used is $N_e \approx 50 \pm 5$ monomer units [51]. The chains we model have $N = 2^{18} = 262144$ units confined in a cubic volume of the size of $44 \times 44 \times 44$ reduced DPD units with periodic boundary conditions. Note that in a such a long chain ($N/N_e \simeq 5000$) the equilibration time for a globule exceeds by far the times accessible in computer simulation, so the choice of the starting configurations plays a very significant role. Here we provide a short outline of how we construct and prepare the initial states of the globules we model, addressing the reader to [32] for full details.

The first initial state we use is a randomized Moore curve similar to that described in [11], it has a very distinct domain structure with flat domain walls. The second initial state is generated by a mechanism which we call the conformation-dependent polymerization in poor solvent. This algorithm, which, for the best of our knowledge, has never been suggested before, is constructing the chain conformation by consecutively adding monomer units in a way that they tend strongly to stick to the

already existing part of the chain. In [32] we show that the resulting conformations show exactly the statistical characteristics (fractal dimensionality, domain structure, absence of entanglements) expected from fractal globules. In what follows, for brevity we call the globule prepared by the randomized Moore algorithm ‘‘Moore’’, and one prepared by the conformation-dependent polymerization ‘‘random fractal’’. As a control sample we use a standard equilibrium globule which we call ‘‘Gaussian’’.

Prior to the diffusion measurements all three initial states are annealed for $\tau = 3.2 \times 10^7$ modeling steps. The statistical properties of random fractal and Gaussian globule does not change visibly during the annealing time, while the Moore globule is evolving with domain walls roughening and its statistical characteristics (e.g., the dependence of the spatial distance between monomers on the genomic distance $\langle r^2(s) \rangle$), see [32]) approach those for the random fractal globule state.

We show the snapshots of the chains modeled by different techniques in Fig.1. Fractal states are characterized by the existence of territorial domains of the same color (i.e., close along the chain) and the compactness of the domains as compared to the Gaussian one. Note also that the overall shape of the Gaussian chain fragment is almost conserved due to the presence of a reptation tube. The three states of the chain are further characterized in Fig.2. The fractal globule curve seems to be very similar (but for the saturation at high s due to the finite size effects) to the universal spatial size-length curve for unentangled rings reported in [21]. $R^2(s)$ for the Moore state seems to approach the fractal globule curve asymptotically with growing modeling time suggesting the existence of a unique metastable fractal globule state.

Summing up, we prepare fractal globule state by two drastically different techniques. The resulting states are significantly different at first, but they converge with the growing simulation time. In our opinion, convergence of the results obtained starting from these two very different conformations is a strong evidence in support of the fact that our results are generic for fractal globules and not sensitive to the details of the initial state.

After the annealing is finished, we measure the monomer spatial displacement for the next $t = 6.5 \times 10^7$ time steps. The resulting dependences of the average mean-square displacement are shown in figure 3. Impressively, the results for the random fractal and Moore initial states are indistinguishable within the measurement errors. At the same time, they differ clearly from the mean-square displacement in the Gaussian globule state which shows the asymptotic behavior compatible with the predictions of the reptation model. Indeed, the observed scaling exponent for Gaussian globule α_G is fairly close to $\alpha_{\text{ent}} = 1/4$ predicted by the reptation model, while for the fractal globule one gets α_F which clearly is above $\alpha_{\text{ent}} = 1/4$ but below the prediction of the Rouse model $\alpha_R = 1/2$. The numerical result we

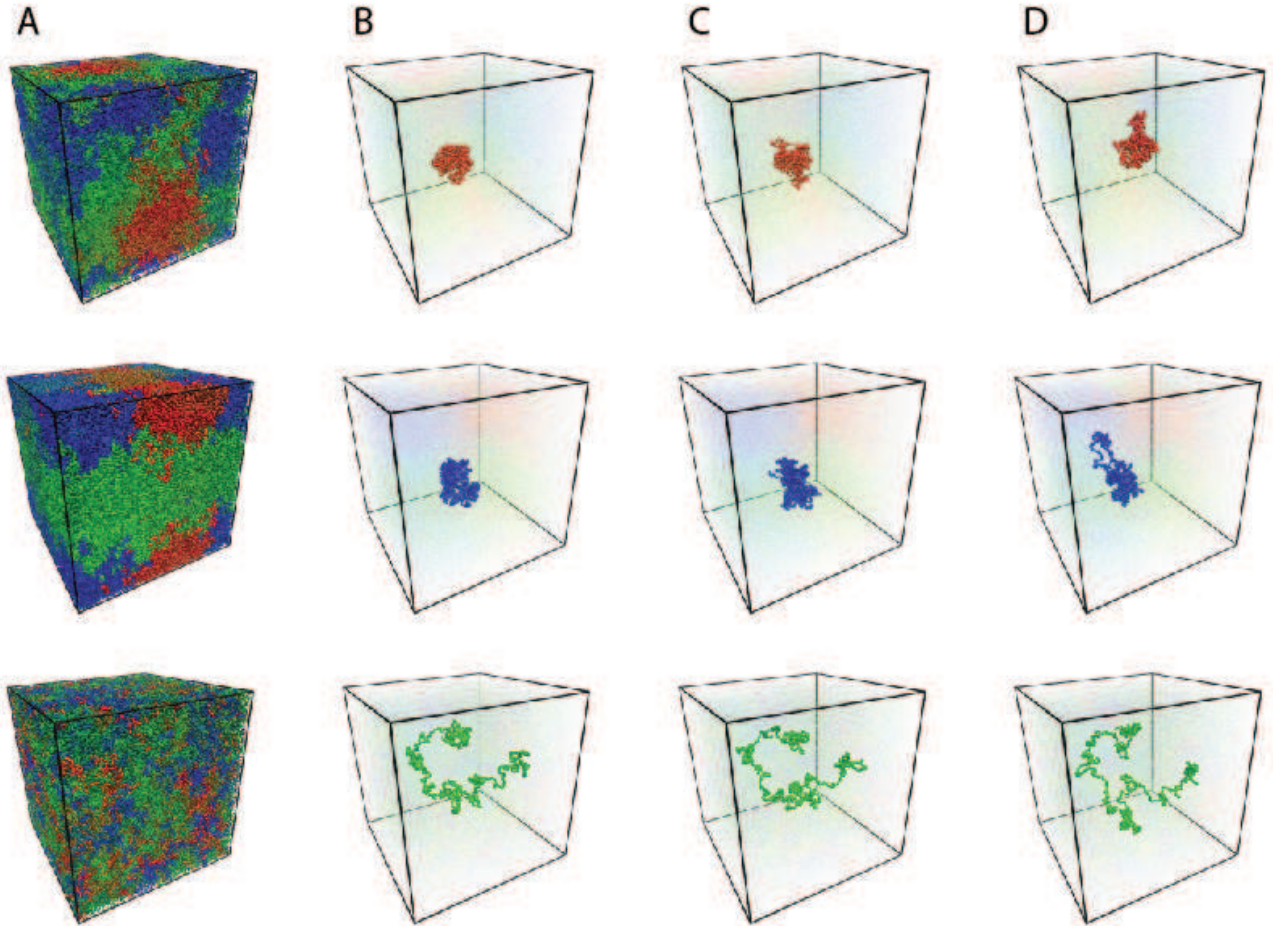


Figure 1: (Color online) The snapshots of globule conformations used in the computer simulations, random fractal globule (top row), Moore globule (middle row), and equilibrium Gaussian globule (bottom row). A): The overall view of the modelling cell at the start of the simulation, after annealing the systems for $2^{25} = 3.2 \times 10^7$ DPD steps. The chain is gradiently colored from one end to another. B)-D): The evolution of a subchain of 1000 monomers during the simulation. B) conformation at the beginning of the simulation after annealing the systems for 3.2×10^7 DPD steps, conformations after simulation for C) $2^{18} \approx 2.5 \times 10^5$ DPD steps, D) $2^{26} \approx 6.5 \times 10^7$ DPD steps.

obtain, $\alpha_F^{exp} \approx 0.38$, is slightly below the theoretical prediction $\alpha_F^{th} = (1 + 3\beta/2)^{-1} = 0.4..0.42$. We expect that this discrepancy may be due to the influence of hydrodynamic interactions in the way similar to [44], however, the quantitative theory to allow for this effect goes beyond the scope of this paper.

The scaling theory introduced can be used, for example, to estimate the first passage time for finding a fixed target within a globule. Since $2/\alpha_F > d$ (d here is the dimensionality of the underlying space and is not to be confused with d_f), we expect the sub-diffusion of monomer units to be recursive [45, 46], and the volume of the space visited by one monomer to grow as

$$V(t) \sim (\langle X^2(t) \rangle)^{d/2} \sim t^{d\alpha_F/2}. \quad (6)$$

Therefore the typical time needed to explore the whole volume of the globule formed by the chain of N monomer

units (which is needed to find a microscopic randomly-placed target) scales as

$$T_{target} \sim V^{2/(d\alpha_F)} \sim N^{(2+\beta d_f)/d_f} \quad (7)$$

$$(2 + \beta d_f)/d_f \approx 1.6$$

Similarly, the typical cyclization time for a subchain of length n (i.e., the typical time needed for the two units separated by a subchain of length n to meet each other in space for the first time, see [47–49]) equals the time needed to explore the volume $v \sim n^{d/d_f}$ and is given by

$$T_{cycl} \sim n^{(2+\beta d_f)/d_f} \approx n^{1.6} \quad (8)$$

Note, that this time is much smaller than the typical Rouse time $T_R = n^2$, which regulates cyclization of a Gaussian polymer coil in a viscous environment, not to mention the typical time needed for the units of an entangled globule to find each other (in the entanglement-controlled case $N_e < n < N^{2/3}$ it can be estimated as

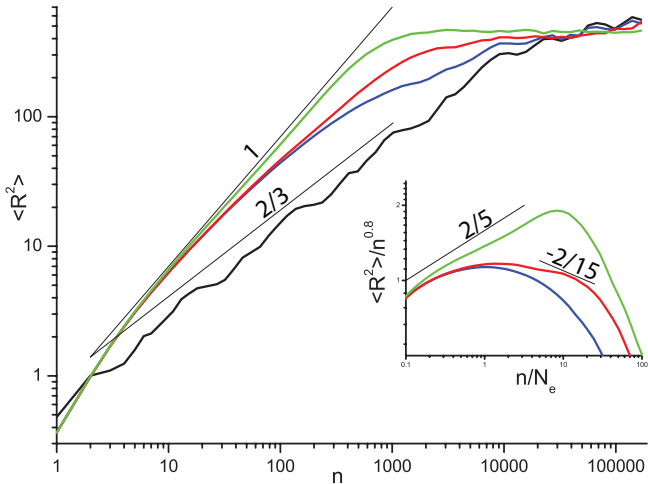


Figure 2: (Color online) The dependences of mean-square distance $\langle R^2 \rangle$ between the monomers as a function of distance along the chain n . Different colors correspond to different initial states, Gaussian (green) and random fractal (red) states are stable on the modeling timescale (see Figure 2 in [32]). The initial Moore state corresponds to the black curve, while the annealed (after 3.2×10^7 DPD steps) Moore state is described by the blue one, which seems to be approaching the random fractal state. Inset shows the same plots in rescaled coordinates $\langle R^2 \rangle n^{-0.8}, n/N_e$ used in [21]. The rapid decline for large n corresponds to the saturation of the graphs in the main plot and is due to the finite-size effects.

$T_{\text{ent}} \sim n^{2/(d_f \alpha_{\text{ent}})} \sim n^4$, where $d_f = 2$ due to the Flory theorem [4]). Therefore, we see that fractal globule state is in this sense advantageous: it takes monomers less time to find each other in this state, thus enhancing the speed of gene regulation processes. We consider this to be an additional argument in favor of the fractal globule model of genome packing.

In conclusion, let us emphasize the two most important results of this letter concerning the stability and dynamics of a fractal globule. First, we suggest the existence of a unique metastable fractal globule state and suggest a novel algorithm to construct this state in computer experiment. We show that an artificially regular fractal globule state constructed in a conventional way as a randomized Moore curve [11] converges after annealing to the same unique state. Second, we show both analytically and numerically that the self-diffusion in a fractal globule state, while much faster than that in the entangled equilibrium globule, is not, contrary to a wide-spread opinion, described by a Rouse model, but is a sub-diffusion

with a different characteristic exponent $\alpha_F \approx 0.38..0.42$. This result is supported by both our computer simulations and experimental results [34–36] on the dynamics of chromatin in the nuclei. By analogy with the Rouse model, we expect the dynamics in the fractal globule to be a fractional Brownian motion, but full analysis of this matter goes beyond the scope of the current letter. Finally, we show that the compactness of the domains cou-

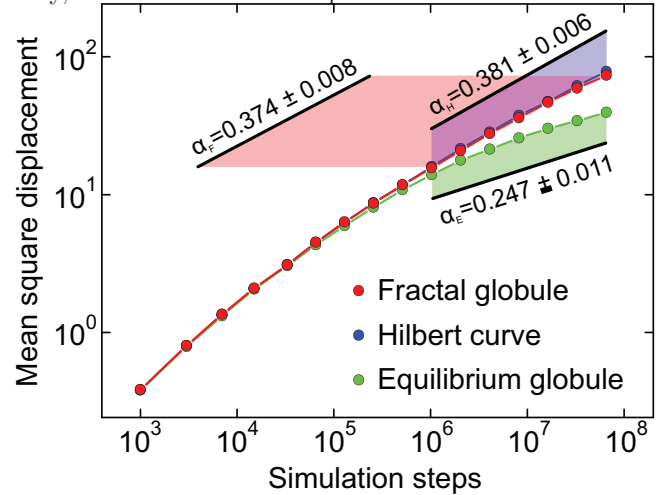


Figure 3: (Color online) Average mean-square displacements of monomer units as a function of time. Globules starting from an irregular fractal (red), regular Gilbert (green), and equilibrium globule (blue) initial conformations. All conformations were annealed for $2^{25} = 3.2 \times 10^7$ timesteps before the measurements started.

pled with comparatively fast subdiffusion leads to the estimate $T \sim n^{1.6}$ for the time at which two monomers first meet each other, which is substantially faster than the Rouse time $T \sim n^2$, not to mention the first passage time in the entangled melt. We suggest that this ability of different parts of chromatin to find each other fast is crucial for fast regulation of gene expression. Further analysis of the first passage time for the fractal globules will be provided elsewhere [50].

The authors are grateful to V. Avetisov, A. Grosberg, M. Imakaev, S. Majumdar, R. Metzler, A. Mironov, S. Nechaev, E. Kepten, A. Semenov, K. Snappen, and R. Voituriez for many illuminating discussions on the subject of this work. This work is partially supported by the IRSES project FP7-PEOPLE-2010-IRSES 269139 DCP-PhysBio, the RFBR grant 14-03-00825, and the SkolTech seed grant.

- [1] T. Cremer and C. Cremer, Nature review Genetics, **2**, 292 (2001).
 [2] B. Alberts, A. Johnson, J. Lewis, M. Raff, K. Roberts, and P. Walter, Molecular Biology of the Cell, 5th edition, Garland Science, NY, 2008.

- [3] P.-G. de Gennes, Scaling Concepts in Polymer Physics, Cornell University Press, NY, 1979.
 [4] A.Yu. Grosberg, A.R. Khokhlov, Statistical Physics of Macromolecules, AIP Press, NY, 1994.
 [5] A. Rosa, R. Everaers, PLoS Computational Biology, **4**:

- e1000153 (2008).
- [6] R.K. Sachs, G. van der Engh, B. Trask, H. Yokota, and J.E. Hearst, *Proc. Nat. Acad. sci.*, **92**, 2710 (1995).
- [7] C. Münkkel, and J. Langowski, *Phys. Rev. E*, **57**, 5888 (1998).
- [8] J. Ostashevsky, *Mol. Biol. of the Cell*, **9** 3031 (1998).
- [9] J. Mateos-Langerak, M. Bohn, W. de Leeuw, O. Giromus, E. M. M. Manders, P. J. Verschure, M. H. G. Indemans, H. J. Gierman, D. W. Heerman, R. van Driel, and S. Goetze, *Proc. Nat. Acad. Sci.*, **106**, 3812 (2009).
- [10] B.V.S. Iyer, and G. Arya, *Phys. Rev. E*, **86**, 011911 (2012).
- [11] M. Barbieri, M. Chotalia, J. Fraser, L.-M. Lavitas, J. Dostie, A. Pombo, and M. Nicodemi, *Proc. Nat. Acad. Sci.*, **109**, 16173 (2012).
- [12] A.Y. Grosberg, Y. Rabin, S. Havlin, and A. Neer, *Europhys. Lett.* **23** 373 (1993)
- [13] E. Lieberman-Aiden, N.L. van Berkum, L. Williams, M. Imakaev, T. Ragozcy, A. Telling, I. Amit, B.R. Lajoie, P.J. Sabo, M.O. Dorschner, *et al*, *Science* **326**, 289 (2009)
- [14] L.A. Mirny, *Cromosome Res.* **19**, 37 (2011)
- [15] A.Yu. Grosberg, S.K. Nechaev and E.I. Shakhnovich, *J. de Physique* **49**, 2095 (1988)
- [16] S.K. Nechaev, A.Yu. Grosberg, and A.M. Vershik, *J. Phys. A: Math. and Gen.*, **29** 2411 (1996).
- [17] S. Nechaev and O.Vasilyev, *Journal of Knot theory and Its Ramifications*, **14**, 243 (2005)
- [18] M. Cates and J. Deutsch, *J. de Physique*, **47**, 2121 (1986)
- [19] T. Sakaue, *Phys. Rev. Letters*, **106**, 167802 (2011)
- [20] T. Sakaue, *Phys. Rev. E*, **85**, 021806 (2012)
- [21] J.D. Halverson, G.S. Grest, A.Y. Grosberg, and K. Kremer, *Phys. Rev. Letters*, **108**, 038301 (2012).
- [22] A.Yu. Grosberg, *Soft Matter*, **10**, 560 (2014)
- [23] J. Bridger and E. Volpi, eds., *Fluorescence in situ Hybridization (FISH): Protocols and Applications*, vol. 659 (Humana Press Inc., Totowa, NJ, 2010).
- [24] J. Dekker, K. Rippe, M. Dekker, and N. Kleckner, *Science* **295** 1306 (2002)
- [25] J.E. Dixon, S. Selvaraj, F. Yue, A. Kim, Y. Li, Y. Shen, M. Hu, J.S. Liu, and B. Ren, *Nature* **485** 376 (2012)
- [26] T. Sexton, E. Yaffe, E. Kenigsberg, F. Bantignies, B. Leblanc, M. Hoichman, H. Parrinello, A. Tanay, and G. Cavalli, *Cell* **148** 458 (2012)
- [27] Y. Zhang, R.P. McCord, Y.-J. Ho, B.R. Lajoie, D.G. Hildebrand, A.C. Simon, M.S.Becker, F.W. Alt, and J. Dekker, *Cell* **148** 908 (2012)
- [28] J.P. Wittmer, H. Meyer, A. Johnner, S. Obukhov, and J. Baschangel, *J. Chem. Phys.*, **139**, 217101 (2013).
- [29] R.D. Schram, G.T. Barkema, and H. Schiessel, *J. Chem. Phys.*, **138**, 224901 (2013).
- [30] A. Rosa, R. Everaers, arXiv: 1310.7641.
- [31] J. Smrek and A.Yu. Grosberg, *Physica A*, **392**, 6375 (2013)
- [32] M.V. Tamm, L.I. Nazarov, A.A. Gavrilov, and A.V. Chertovich, supplementary materials to this paper, see below.
- [33] M. Imakaev, L.Mirny, *Book of Abstracts of the Moscow Conference on Computational Molecular Biology*, 141 (2011).
- [34] I. Bronstein, Y. Israel, E. Kepten, S. Mai, Y. Shav-Tal, E. Barkai, and Y. Garini, *Phys. Rev. Let.*, **103**, 018102 (2009).
- [35] K. Burnecki, E. Kepten, J. Janczura, I. Bronstein, Y. Garini, and A. Weron, *Biophys. Journal*, **103**, 18391847 (2012).
- [36] E. Kepten, I. Bronstein, and Y. Garini, *Phys. Rev. E*, **87**, 052713 (2013).
- [37] M. Doi, S.F. Edwards, *The Theory of Polymer Dynamics*, Oxford University Press, Oxfrd, 1986.
- [38] J.D. Halverson, J. Smrek, K. Kremer, and A.Yu. Grosberg, arXiv:1311.5262.
- [39] J.D. Halverson, W.B. Lee, G.S. Grest, A.Yu. Grosberg, and K. Kremer, *J. Chem. Phys.*, **134**, 204904 (2011).
- [40] Y. Kantor and M. Kardar, *Phys. Rev. E*, **76** 061121 (2007); C. Chatelain, Y. Kantor, and M. Kardar, *Phys. Rev. E*, **78** 021129 (2008)
- [41] R.D. Groot, P.B. Warren, *J. Chem. Phys*, **107**, 4423 (1997)
- [42] P. Nikunen, I. Vattulainen, and M. Karttunen, *Phys. Rev. E*, **75**, 036713 (2007)
- [43] A. Karatrantos, N. Clarke, R.J. Compostob, and K.I. Wineyb, *Soft Matter*, **9**, 3877 (2013) and references therein.
- [44] J. Farago, H. Meyer, and A.N. Semenov, *Phys. Rev. Let.*, **107**, 178301 (2011).
- [45] B. H. Hughes, *Random Walks and Random Environments*, vol. 1, Clarendon Press, Oxford, 1996
- [46] O. Bénichou, C. Chevalier, J. Klafter, B. Meyer, and R. Voituriez, *Nature Chemistry*, **2**, 472 (2011)
- [47] G. Wilemski and M. Fixman, *J. Chem. Phys.*, **60** 866; 878 (1974).
- [48] A.E. Likhtman and C.M. Marques, *Europhys. Letters*, **75**, 971 (2006).
- [49] T. Guérin, O. Bénichou, and R. Voituriez, *Nature Chemistry*, **4**, 568 (2013).
- [50] M.V. Tamm, L.I. Nazarov, A.A. Gavrilov, and A.V. Chertovich, in preparation.
- [51] We use the method described in[43] to determin N_e , the referred value corresponds to the so-called s-coil definition of N_e .

Appendix A: Supplementary 1. Dissipative particle dynamics

Dissipative particle dynamics (DPD) is a version of the coarse-grained molecular dynamics adapted to polymers and mapped onto the classical lattice Flory-Huggins theory [1–4]. Consider an ensemble of particles (beads) obeying Newton’s equations of motion

$$\frac{d\mathbf{r}_i}{dt} = \nu_i, m_i \frac{d\nu_i}{dt} = \mathbf{f}_i \quad (\text{A1})$$

$$\mathbf{f}_i = \sum_{i \neq j} (\mathbf{F}_{ij}^b + \mathbf{F}_{ij}^c + \mathbf{F}_{ij}^d + \mathbf{F}_{ij}^r), \quad (\text{A2})$$

where \mathbf{r}_i , m_i , ν_i are the coordinate, mass, and velocity of an i -th bead, respectively, \mathbf{f}_i is the force acting on it. The summation is performed over all other beads within the cut-off radius r_c . Below we assume that all quantities entering Eq. (2,3) are dimensionless and for simplicity set r_c and m_i for any i to unity.

First two terms in the sum (A2) are conservative forces. Macromolecules are represented in terms of the bead-and-spring model. \mathbf{F}_{ij}^b is a spring force describing chain connectivity of beads:

$$\mathbf{F}_{ij}^b = -K(r_{ij} - l) \frac{dr_{ij}}{dr_{ij}}, \quad (\text{A3})$$

where K is a bond stiffness, l is the equilibrium bond length. If beads i and j are not connected, then $\mathbf{F}_{ij}^b = 0$. \mathbf{F}_{ij}^c is a soft core repulsion between i - and j -th beads:

$$\mathbf{F}_{ij}^c = \begin{cases} a_{ij}(1 - r_{ij})\mathbf{r}_{ij}/r_{ij}, & r_{ij} \leq 1 \\ 0, & r_{ij} > 1 \end{cases} \quad (\text{A4})$$

where a_{ij} is a maximum repulsion between beads i and j attained at $r_i = r_j$. Since \mathbf{F}_{ij}^c has no singularity at zero distance, a much larger time step than in the standard molecular dynamics could be used.

Other, non-conservative, constituents of \mathbf{f}_i are a random force \mathbf{F}_{ij}^r and a dissipative force \mathbf{F}_{ij}^d , acting as a heat source and medium friction, respectively. They are taken as prescribed by the Groot-Warren thermostat in [4].

It was shown[5, 6] that the DPD method is consistent with both the scaling theory of polymers (e.g., it gives correct relationships between the average radius of gyration of a coil and the number of units in the coil) and the Rouse dynamics.

The use of soft volume and bond potentials leads to the fact that the bonds are formally “phantom”, i.e. capable of self-intersecting in three dimensions. The phantom nature of chains does not affect the equilibrium properties (for example, the chain gyration radius or the phase behavior of the system); moreover, it greatly speeds up the equilibration of the system. However, the dynamical properties of the chains, such as the self-diffusion or the features requiring explicit account for the entanglements between chains, are, of course, dependent on whether the chain is phantom or not, making the situation more subtle. It is necessary therefore to introduce some additional forces that forbid the self-intersection of the bonds. These forces are usually quite cumbersome and considerably slow in computation. Nikunen et al. [7] described a method for turning chains nonphantom in DPD without introducing any addition forces. It is based on geometrical considerations: if any two units in the system cannot approach each other closer than r_{\min} , every unit in the system effectively has an excluded radius of $r_{\min}/2$. If it also assumed that each bond has a maximum length l_{\max} , the condition of self-avoiding chains is $\sqrt{2}r_{\min} > l_{\max}$.

Although particles in DPD are formally pointlike, they have an excluded volume due to the presence of the repulsive potential at any nonzero value of a_{ij} . Similarly,

the existence of a bond potential causes the bond to have a maximum possible length.

In our study, we chose $a_{ij} = 150$, $l = 0.5$, and $K = 150$. The other parameters are: DPD number density $\rho = 3$; noise parameter $\sigma = 3$; integration timestep $\Delta t = 0.03$.

Appendix B: Supplementary 2. Initial states

In our work we use three different ways to construct initial states of globules which we describe below in detail. In all cases chain of $2^{18} = 262144$ monomers are generated in a cubic box with periodic boundary conditions, the size of the modelling box is $44 \times 44 \times 44$ reduced DPD units, making the average number density of monomers equal to $\rho = 3$ (this value is known[?]] to be especially good for modelling the dynamic properties of polymer chains). All three initial states are constructed on a cubic lattice with lattice constant equal to $3^{-1/3} \approx 0.69$ and after the construction are allowed to anneal for $2^{25} = 3.2 \times 10^7$ DPD time steps. Only after this annealing the self-diffusion measurements are started.

1. Random fractal globule

The idea of this mechanism to design a fractal globule state, which we propose here for the first time, is based on the following considerations. Imagine a polymer chain being synthesized while being in a poor solvent, in a way that all the already synthesized part is forming a tight globule. Assume also the synthesis to be very fast as compared to the internal movements of monomers within a globule. In that way one expects that at all intermediate stages the already formed part of the globule is in a compact state. Also one expect that formation of knots and entanglements will be highly suppressed since the new monomers are mostly to the surface of the existing globule, and cannot go through it as there are no holes left in the structure. Clearly, the conformation thus formed is very reminiscent of a fractal globule.

To exploit this idea we proceed as follows. We construct the polymer conformation as a trajectory of a lattice random walk in a potential strongly attracting the walker to the places it has already visited. At each step a walker on a cubic lattice has 6 neighboring cites (see Figure 4) where he can possibly move. We postulate the probability to go at each of the possible target cites to depend on whether it was already visited, and on how many visited cites it has as its neighbors. In particular,

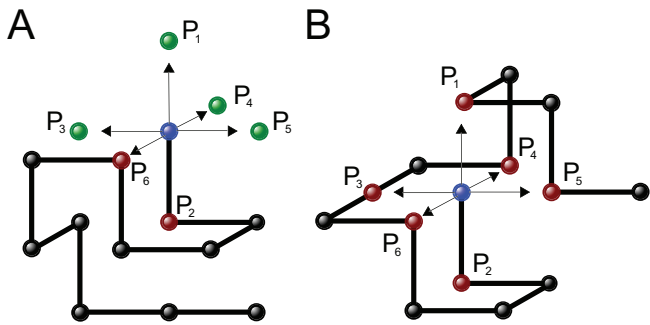


Figure 4: The conformation-dependent random walk. (A) on the next step the probabilities of choosing steps 3 and 5 are large compared to steps 1 and 4 ($P_4 = P_1$; $P_3 = (1 + 2A)P_1 = 20001P_1$, $P_5 = (1 + A)P_1 = 10001P_1$, probabilities of steps 2 and 6 are proportional to ε and are essentially zero; (B) trapped configuration: weights of all possible steps equal ε and are equiprobable.

we use the following assumptions:

$$P_i = \mathcal{N}^{-1} \begin{cases} \varepsilon & \text{if the target cite is visited,} \\ 1 + A \left(\begin{array}{l} \# \text{ of visited neighbors} \\ \text{the target cite have} \end{array} \right) & \text{if the target cite is not visited,} \end{cases}$$

$$\mathcal{N} = \sum_{i=1..6} P_i \quad (\text{B1})$$

Here, ε should be extremely small so that double visiting of the same cites should be possible only if the walk gets locked (we use $\varepsilon = 10^{-9}$), while A is a constant defining the strength of attraction to the existing trajectory, and should therefore be large to keep all the intermediate conformations compact. By trial and error we have found $A = 10,000$ to work best.

A trajectory constructed in this way includes a finite fraction (of order of several percent) self-intersections. However, the resulting states happens to be almost unknotted:

The segment of 10^4 monomers is reduced to a knot of less than 10^2 monomers. For comparison, a segment of an equilibrium globule of 10^4 monomers is reduced to a knot of $2 \cdot 10^3$ points.

To characterize the resulting states we studied the spatial distance as a function of distance along the chain, and the return probability of the chain (see Fig.6 and Fig.2 of the main text, see also Fig.2 of the main text for the snapshots of the state). One more important question is whether the characteristics of the resulting conformations are stable along the chain: indeed, the rules generating the conformation are asymmetric (the walker is attracted to the sites he visited in the past, but not to the sites he will visit in the future), so one can expect

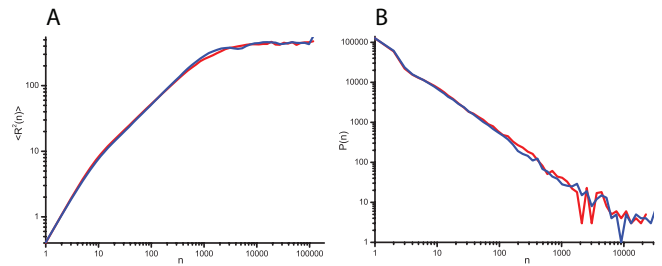


Figure 5: Characterization of the first (red) and second (blue) halves of the chain generated by the conformation-dependent polymerization algorithm. A) the average spatial distance between monomers $\langle R^2(n) \rangle$ as a function of the chemical distance between them n , B) the non-normalized return probability $P(n)$ (number of monomers which happen to be spatially adjacent while being separated by chemical distance n).

the start and end parts of the chain to behave differently. To check that, we calculated the average distance between monomers $\langle R^2(n) \rangle$ and the return probability $P(n)$ separately averaged over the first and the last half of the chain. The results are shown in Fig.???. One sees that amazingly there seems to be no bias, and the first and second halves of the chain behave exactly the same within experimental error.

The characteristics of thus constructed conformations are, thus, exactly similar to what one expects of a fractal globule conformations, and moreover, as shown in Fig.6(A,D) they appear to be very stable throughout the modelling timescale.

In our opinion, the fractal conformations constructed by conformation-dependent polymerization described above are not only useful for fast generation of fractal states, but are of fundamental as well as practical interest. We plan to study them further and in more detail elsewhere [8]

2. Moore curve

Moore curve is an example of a class of recursively defined space-filling curves whose various definitions go back to the end of 19th century[9, 10]. On the first iteration step consider a curve passing through the cube vertexes as shown in Fig.7(A). The next iteration consist of i) swelling up the 1-st iteration curve by a factor of 2, ii) replacing each “swollen” vertex of the curve with a $2 \times 2 \times 2$ cube, iii) filling up this newly formed cubes by replicas of the original 1-st iteration curve rotated in a way to preserve the connectivity of the curve as a whole (see Fig.7 (B)). Then this procedure can be repeated again and again - swelling up the existing curves and replacing each node with a $2 \times 2 \times 2$ subcube whose nodes are circumented by a curve identical to the 1st iteration curve rotated in the way to preserve overall connectivity of the picture.

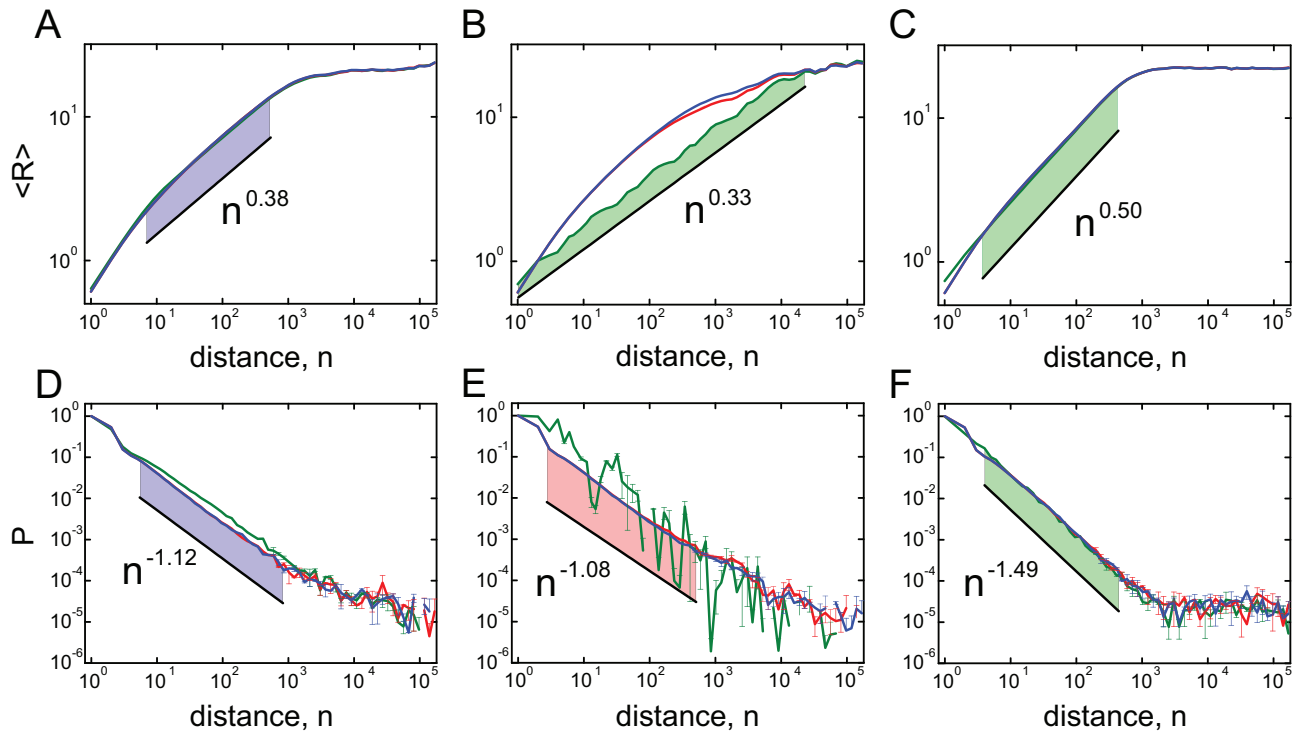


Figure 6: The dependence of the average root-mean squared distance $R(n) = \sqrt{\langle R^2(n) \rangle}$ between monomers and return probability $P(n)$ on the genomic distance n between monomers for three initial states under study: (A, D) the random fractal globule, (B, E) the randomized Moore curve, (C, F) the equilibrium Gaussia globule obtained by the loop-exchange algorithm. Green curves correspond to initial states, red curves - to the states obtained after annealing for $2^{25} \approx 3.2 \times 10^7$ DPD steps, blue curves - to the final states in the end of the modelling, i.e. after $3 \times 2^{25} \approx 9.7 \times 10^7$

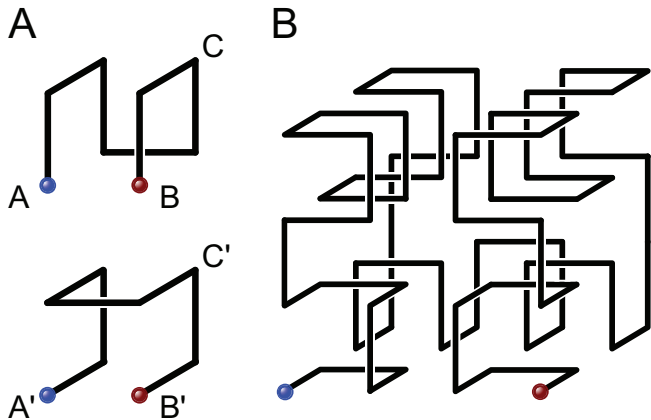


Figure 7: The space-filling curve design: (A) first iteration of the construction. There are two mirror-symmetrical ways to circumvent the $2 \times 2 \times 2$ designated ACB and $A'C'B'$, respectively; (B) second iteration of the construction: ABC curve is swollen by a factor of two, each node replaced by a $2 \times 2 \times 2$ subcube and all subcubes are circumvented according to the $A'B'C'$ curve.

Different ways of constructing space-filling curves (there are Peano version, Hilbert version, etc.) differ by the exact details of the iteration procedure. Note that

in the Moore procedure described above there are two mirror-symmetrical ways to choose the initial curve of first iteration, as shown in Fig.7(A). Consequently, there exist some ambiguity in choosing the particular configuration: indeed, on each iteration step, when replacing a node with a fragment of curve visiting vertices of a $2 \times 2 \times 2$ subcube it is possible to choose (independently each time) one of the two mirror-symmetrical ways to circumvent the nodes.

In simulations we deal with two realizations of a space-filling curve Moore curves formed after 6 iterations and consisting of $(2 \times 2 \times 2)^6 = 262144$ nodes. One conformation is a “stereo-regular” Moore curve with some particular choice of mirror-symmetric variants. Another allows the choice of “stereo isomers” shown in Fig.7A at random (this procedure is very similar to one described in [11]). This leads to a conformation with same statistical characteristics but different intra-chain contacts. We have not noticed any measurable difference in the long-range statistics and evolution of these states, so under label ‘Moore’ in the main text we provide the results averaged over these two realizations.

Remarkably, as these initial states anneal, their characteristics seem to relax towards those of a fractal globule state described above, see Fig.6(B,E).

3. Equilibrium globule

Since the full relaxation time of a globule goes far beyond the time-scales available at our simulations, we have to use some special trick to obtain a reference equilibrium globule conformation with Gaussian statistics of the short chain fragments. To do that we proceed as follows. We start with a Moore curve described in the previous subsection and then let it undergo a loop transfer algorithm as follows. At each step of the algorithm we i) take an arbitrary pair of units which are adjacent on the lattice but not along the chain (shown in red in Fig.8(B)) and switch the links between these units in a way shown in Fig.8(B), as a result the chain fragment between these two units is “cut out” and form a separated loop. Then, ii) we go along this newly formed loop and choose an arbitrary link of it (between monomers shown in blue in Fig.8(C) which is adjacent and parallel to a link of the original chain and perform another links switch as shown in Fig.8(C) to insert the loop into a different place of the original chain. Such a loop transfer preserves the total chain length and the uniform density over the entire volume, but allows a significant change of the conformation topology. After repeating this procedure many times (of the order of the total number of chain links, by trial and error we found that 5×10^4 successful transfer steps is

sufficient for our chain-length) we obtain a lattice conformation which is connected and uniform in space but otherwise completely random. Indeed, one can see that the dependence of an average spatial distance between two monomers $\langle R(n) \rangle$ on a distance between them along the chain n is transformed into the dependence which is typical for the equilibrium globule state, i.e.

$$\begin{aligned} \langle R(n) \rangle &\sim n^{1/2} && \text{for } n < N^{2/3}; \\ \langle R(n) \rangle &\sim \text{const} && \text{for } n > N^{2/3}, \end{aligned} \quad (\text{B2})$$

see Fig.6(C), the contact probability $P(n)$ also changes to one typical for Gaussian chains:

$$\begin{aligned} P(n) &\sim n^{-3/2} && \text{for } n < N^{2/3}; \\ P(n) &\sim \text{const} && \text{for } n > N^{2/3}, \end{aligned} \quad (\text{B3})$$

see Fig.6(F).

Throughout the modelling the statistical properties of thus obtained equilibrium knotted state remain constant (see Fig.6(C,F)).

We find this loop transfer algorithm of producing an equilibrium knotted state with a uniform density in a cubic volume to be very simple, fast and useful.

-
- [1] P.J. Hoogerbrugge, and J.M.V.A. Koelman, *Europhys. Lett.*, **19**, 155 (1992).
 - [2] A.G. Schlijper, P.J. Hoogerbrugge, and C.W. Manke, *J. Rheol.*, **39**, 567 (1995).
 - [3] P. Espanol, and P.B. Warren, *Europhys. Lett.*, **30**, 191 (1995).
 - [4] R.D. Groot, and P.B. Warren, *J. Chem. Phys.*, **107**, 4423 (1997).
 - [5] N.A. Spenley, *Europhys. Lett.*, **49**, 534 (2000).
 - [6] F. Lahmar, and B. Rousseau, *Polymer*, **48**, 3584 (2007).
 - [7] P. Nikunen, I. Vattulainen, and M. Karttunen, *Phys. Rev. E*, **75**, 036713 (2007).
 - [8] L.I. Nazarov, M.V. Tamm, S.K. Nechaev, in preparation.
 - [9] G. Peano, *Math. Ann.*, **36**, 157 (1890).
 - [10] D. Hilbert, *Math. Ann.*, **38**, 459 (1891).
 - [11] R.D. Schram, G.T. Barkema, and H. Schiessel, *J. Chem. Phys.*, **138**, 224901 (2013).

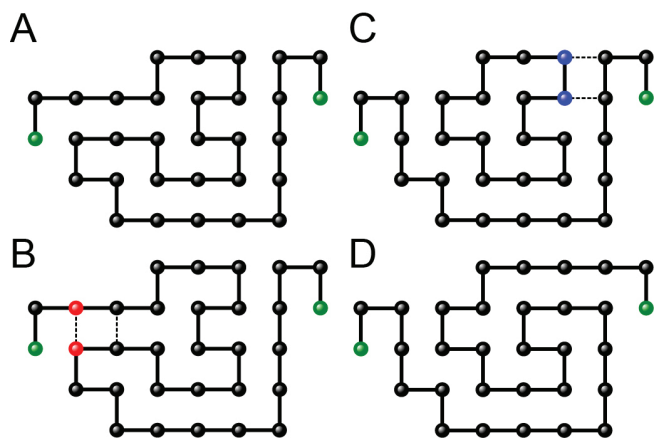


Figure 8: The scheme of a loop-transmission algorithm. A) The initial conformation of the chain; B) first bond switching, formation of a separate loop; C) intermediate state with a separate loop and second bond switching; D) the resulting polymer conformation.